Assignment 5

CASPER BRESDAHL, whs715, University of Copenhagen, Denmark

1 INTRODUCTION

This week we will look at how to apply the Finite Element Method to the Cauchy equation. We will then look at two experiments. The first looking at the elasticity of different materials and how the area of our beam changes as we apply pressure to it. The second looks at how the grid resolution impacts our approximation.

2 THEORY

We will now look at a 2D elasticity problem. The elasticity of a material is its ability to resist a distorting effect which would deform it, and to return to its original size and shape when the distorting force is removed. To get a better understanding of elasticity we will now apply the Finite Element Method (FEM) to the Cauchy Equation: $\rho\ddot{x} = \nabla \cdot \sigma + b$, where ρ is the spatial mass density, $\ddot{x}$ is the spatial acceleration, $\nabla \cdot \sigma$ is the divergence of the Cauchy stress tensor where the Cauchy stress tensor is defined by the Cauchy's stress hypothesis: $t = \sigma n$. Here n is the unit normal vector to a plane and t is the corresponding traction on the plane. Conservation of angular momentum implies σ is symmetric. Lastly b is body force. The Cauchy Equation is the continuum mechanics equivalent of Newtons second law which state that the change of momentum of a body over time is directly proportional to the force applied, and it occurs in the same direction as the applied force. We can now apply the five steps of FEM.

Step 1: The first step of FEM is to rewrite the Cauchy Equation to a volume integral. We do this by moving the terms around a little, multiply by our test function and taking the integral. This gives us:

$$\int_{\Omega} (\rho\ddot{x} - \nabla \cdot \sigma - b)^T w d\Omega = 0$$

Where w is our test function. This integral is in the spatial domain, and thus is time variant. This means Ω changes for every time step. As this is quite impractical, we instead prefer to integrate over the material coordinates. We can go from the spatial coordinates to material coordinates because the spatial coordinates is a deformation of the material coordinates. After the change of coordinates, the above equation becomes:

$$\int_{\Omega_0} (\rho\ddot{x} - \nabla \cdot \sigma - b)^T w j d\Omega_0 = 0$$

Where j is the determinant of the deformation gradient. As we are dealing with a quasi-static problem we will now assume $\ddot{x} = 0$, and we will also assume we are dealing with small displacements, that means our spatial and material coordinates are almost identical, which allows us to define $j = 1$. This means we end with the new equation:

$$\int_{\Omega_0} (-\nabla \cdot \sigma)^T w d + \Omega_0 \int_{\Omega_0} -b^T w d\Omega_0 = 0$$

Author's address: Casper Bresdahl, whs715, University of Copenhagen, Copenhagen, Denmark, whs715@alumni.ku.dk.

Step 2: We can now apply integration by parts. This involves the tensor equivalent to the chain rule which gives us:

$$\nabla \cdot (\sigma w) = (\nabla \cdot \sigma)^T w) + \sigma : \nabla w^T \leftrightarrow$$
$$-(\nabla \cdot \sigma)^T w) = \sigma : \nabla w^T - \nabla \cdot (\sigma w)$$

Substituting with this gives us the equation:

$$\int_{\Omega_0} \sigma : \nabla w^T d\Omega_0 - \int_{\Omega_0} \nabla \cdot (\sigma w) d\Omega_0 - \int_{\Omega_0} b^T w d\Omega_0 = 0$$

We can now also apply the Gauss divergence theorem to rewrite the integral of $\nabla \cdot (\sigma w)$:

$$\int_{\Omega_0} \nabla \cdot (\sigma w) d\Omega_0 = \int_{\Gamma_0} w^T t d\Gamma_0 = \int_{\Gamma_t} w^T t d\Gamma_0$$

Where Γ_0 denotes the boundary in material coordinates and Γ_t denotes the boundary where we apply traction. We have the last equality because the integral over the boundary where we do not apply traction simply becomes zero. Due to the symmetry of σ the symmetric part of ∇w^T will look a lot like the Euler strain tensor, hence we define $\epsilon_w = \frac{1}{2}(\nabla w + \nabla w^T)$. We now have the equation:

$$\int_{\Omega_0} \sigma : \epsilon_w d\Omega_0 - \int_{\Gamma_t} w^T t d\Gamma_0 - \int_{\Omega_0} b^T w d\Omega_0 = 0$$

In **step 3** we now make an approximation of our displacement field $\bar{u}$ which we would like to solve for. We define $\bar{u} = N^e \bar{u}^e$ where N is our shape function, more concretely we will use barycentric coordinates, and the superscript e denotes we are dealing with finite elements. In a 2D problem our mesh would consist of triangles, each with three nodes, i, j and k. We would then sum the nodal values and multiply these with their respective shape function to get our approximation of the displacement field. This can be written as $\bar{u} = \sum_{\alpha \in \{i,j,k\}} N^e_\alpha \bar{u}^e_\alpha$. In **step 4** we can now define our test function as $\bar{w} = N^e \delta \bar{w}^e$ where δ is a random variable. Defining the test function with the use of shape functions is known as the Galerkin method.

Before continuing to the last step we need to convert $\int_{\Omega_0} \sigma : \epsilon_w d\Omega_0$ from tensor notation to vector notation. We know that the stress vector, $\overrightarrow{\sigma}$, is equal to the elasticity matrix, D which is build from the Young's modulus and the Poisson ratio of the material we are modelling, times the strain vector, $\overrightarrow{\epsilon}$. That is, $\overrightarrow{\sigma} = D\overrightarrow{\epsilon}$. And we know $\overrightarrow{\epsilon} = S\bar{u} = SN^e \bar{u}^e$ where S is the differential operator. Defining $B^e = SN^e$ we can now see:

$$\begin{aligned} \sigma : \epsilon_w &= \overrightarrow{\sigma}^T \overrightarrow{\epsilon}_w \\ &= \overrightarrow{\epsilon}^T_w D \overrightarrow{\epsilon}_w \\ &= \delta \bar{w}^{eT} B^{eT} D B^e \bar{u}^e \end{aligned}$$

Substituting all this into our equation we find:

$$\left(\int_{\Omega_0^e} \delta \bar{w}^{eT} B^{eT} D B^e d\Omega_0 \right) \bar{u}^e - \int_{\Gamma_t^e} \delta \bar{w}^{eT} N^{eT} t d\Gamma_0 - \int_{\Omega_0^e} \delta \bar{w}^{eT} N^{eT} b d\Omega_0 = 0$$

We can now move the terms with the random variables outside the integrals and note everything still needs to equal zero, thus we can disregard the terms with random variables. This means we have:

$$\left(\int_{\Omega_0^e} B^{eT} D B^e d\Omega_0\right) \bar{u}^e - \int_{\Gamma_t^e} N^{eT} t d\Gamma_0 - \int_{\Omega_0^e} N^{eT} b d\Omega_0 = 0$$

In **step 5** we can now reduce the terms we have left and compute a solution. In the term $\left(\int_{\Omega_0^e} B^{eT} D B^e d\Omega_0\right) \bar{u}^e$ we note when the shape functions are of first order, then the B terms becomes constant and does not depend on the integral. We thus simply have $B^{eT} D B^e A^e$ where A^e becomes the area of our triangles. In 3D this would be the volume of our tetrahedrals. We can denote this term $\mathbf{K}^e$. The two other integral terms can be combined to a common force vector which we can denote $\mathbf{f}$. This gives us the linear system $\mathbf{K}^e \bar{u}^e = \mathbf{f}^e$. The only thing left to do is to perform the assembly process, apply our boundary conditions and then we can solve for the displacement field.

3 EXPERIMENT 1

In this experiment we would like to test the elasticity and how the area of the beam is preserved when applying varying amounts of force to different materials. We will look at the materials steel, glass, rubber and lead. As our model makes assumptions about small displacements, and all material wants to return to its original shape, we will expect no loss and no gain in area when we apply force. Beginning with steel we can visualize the displacement when applying -10^7 units of force to each node along with a plot of the area of the beam when different amounts of force is applied. The results can be seen in Figure 1.

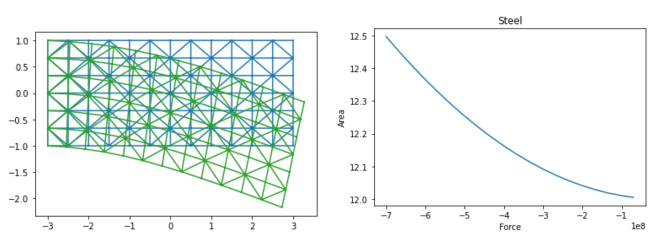

(a) -10^7 units of force applied to steel. (b) Relation between force and area for steel.

Fig. 1. Example of steel displacement together with relation between force and area for steel. Young's modulus is 69^9 and Poisson ratio is 0.3.

We see that the increase in area is somewhat significant and exponentially increasing. Looking at how the bar deforms, we see the topline of the right side not bending, but instead the middle of the bar bending. We can now look at glass which have surprisingly similar Young's modulus and Poisson ratio. The results can be seen in Figure 2.

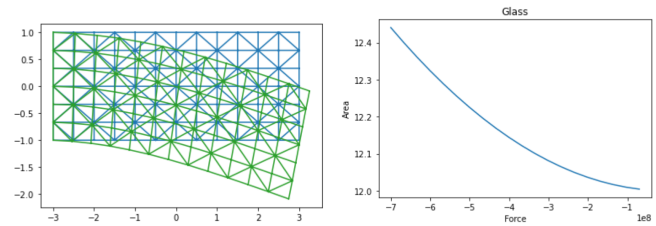

(a) -10^7 units of force applied to glass. (b) Relation between force and area for glass.

Fig. 2. Example of glass displacement together with relation between force and area for steel. Young's modulus is 70^9 and Poisson ratio is 0.22.

We here see similar results where the area changes exponentially, but slightly less than for steel and the beam bends in a natural way. Looking at rubber we have a big decrease in Young's modulus and big increase in Poisson ratio. The results can be seen in Figure 3.

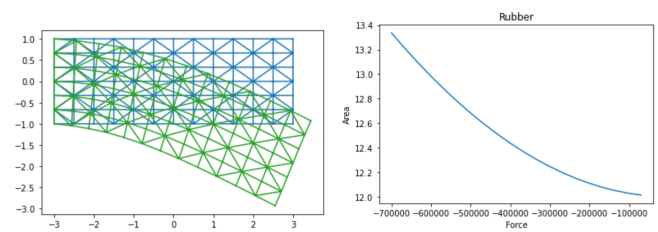

(a) -10^4 units of force applied to rubber. (b) Relation between force and area for rubber.

Fig. 3. Example of rubber displacement together with relation between force and area for steel. Young's modulus is 0.05^9 and Poisson ratio is 0.49.

We here note we need a lot less force to bend the beam, but we still see the same results, exponential increase in area, and the beam bending in a natural way. The last material we will look at is lead and the results can be seen in Figure 4.

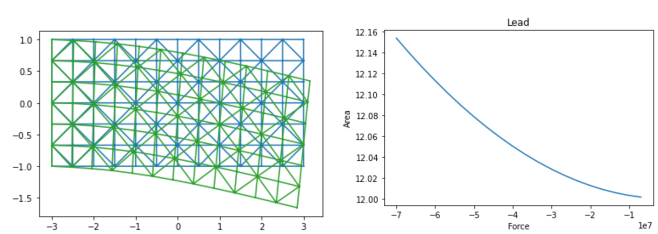

(a) -10^6 units of force applied to lead. (b) Relation between force and area for lead.

Fig. 4. Example of lead displacement together with relation between force and area for steel. Young's modulus is 13.8^9 and Poisson ratio is 0.431.

We again see a natural bend and exponential increase in area.

3.1 Discussion of results

For all material we see an exponential increase in area as we apply force to the beams. As we expected no change in area, we thus conclude our model does introduce some amount of error into our simulation. We can also rank the materials after which we would expect would require the most force to bend. Here We would properly expect steel to require the most force to bend. However, the results shows we need approximately the same force to bend steel and glass. As Young's modulus and Poisson ratio for the two materials are quite close, this is not too surprising. However, I have chosen to go with the assignment value for Young's modulus on steel although some websites put much higher, making steel harder to bend, which would put it in line with our expectation. As we would expect, rubber is the easiest of the four materials to bend, and lead comes in third. The fact the model concurs with our expectation, we conclude we have verified that the model works correctly in this regard.

4 EXPERIMENT 2

In this experiment we would like to examine the effect of grid resolution by looking at the total displacement per grid node and how the area of the beam is conserved. To measure the total displacement per grid node, we will pointwise take each node in the original beam, and compute the norm of the vector to the same node in the displaced beam and then divide by the total number of grid nodes. Summing these displacements will be our total displacement measure. As we increase the grid resolution we would expect the model accuracy to increase, and thus giving us a better approximation to the real solution. However, its hard to say what the 'true' displacement is, and thus we will also measure the area conservation. We will look at the material steel with Young's modulus 69^9 and Poisson ratio 0.3. We will keep the force constant at -10^7. We define our smallest grid resolution as 12 by 6 and then we multiply these sizes by an increasing scaling factor. The results for total displacement per node and area conservation can be seen in Figure 5.

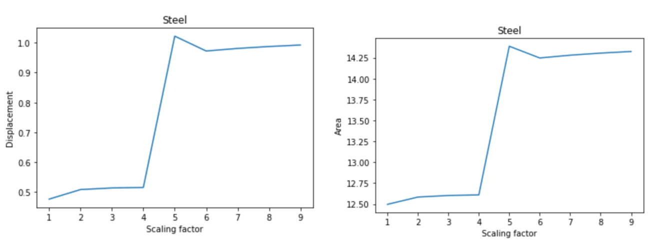

(a) Total displacement per node at different grid resolutions.

(b) Area of beam at different grid resolutions.

Fig. 5. Total displacement per node and area of beam at different grid resolutions at constant force -10^7.

We see that the two graphs are very similar which might not be very surprising as the total displacement of the nodes directly influences the area of the beam. We see that the finer grid resolution we use, the more displacement per node we see, and the more area arise. We also see a big change when the grid resolution becomes 60 by 30, where its like the grid is suddenly 'allowed' to bend in its 'desired' way. We can also take a look at how the beams and their deformation looks. This can be seen in Figure 6.

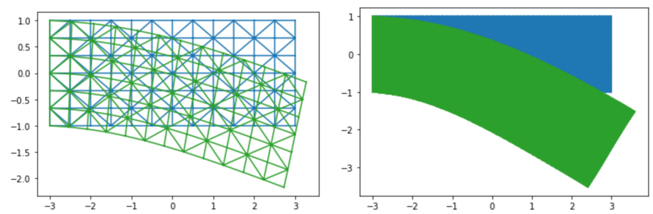

(a) Coarse grid.

(b) Fine grid.

Fig. 6. Coarse and fine grid resolutions at constant force -10^7.

We here clearly see that the displacement is much larger for the finer grid than for the coarse grid as the fine grid has 'sled' all the way down below its original position.

4.1 Discussion of results

From Figure 5 we clearly see the area and total displacement grows drastically when we increase the grid resolution beyond a factor of 5. The sudden increase could indicate we suddenly have enough nodes for a natural deformation as an increase in grid resolution should improve the model accuracy. However, we would still expect the area to be conserved which it is clearly not. We also see that the total displacement per node graph and the area of the beam graph looks very similar. As the two measures are dependent on each other this might not be very surprising, but this could lead one to think the error in the total displacement is then proportional to the error in increasing area. This could lead to an approximation about how the total displacement per node should look like whereas it would be hard to say anything about on its own.

5 CONCLUSION

In conclusion we have seen our model introduces an exponentially increasing error in increased area when we apply force to our beam. On the other hand we can also conclude the 'bend-ability' of our materials in relation to each other are as expected and thus we have verified this part of our model works correctly. We have also looked at the total displacement per grid node and area of the beam when changing the grid resolution. Here we conclude that it is hard to determine how the beam would realistically bend, but we see an increase in both total displacement per node and in area when we increase the grid resolution. The increasing area contradicts our expectation of the model accuracy increasing when increasing the grid resolution. The similarity in the graphs in Figure 5 could also lead one to conclude that the error in total displacement per node is proportional to the error in increased area.